

Synchronization regimes of optical-feedback-induced chaos in unidirectionally coupled semiconductor lasers

A. Locquet,¹ C. Masoller,² and C. R. Mirasso³¹*GTL-CNRS Telecom, UMR CNRS 6603, Georgia Tech Lorraine, 2-3 rue Marconi, 57070 Metz, France*²*Instituto de Física, Facultad de Ciencias, Universidad de la República, Iguá 4225, Montevideo 11400, Uruguay*³*Departament de Física, Universitat de les Illes Balears, E-07071 Palma de Mallorca, Spain*

(Received 5 January 2002; published 29 April 2002)

We numerically study the synchronization of two unidirectionally coupled single-mode semiconductor lasers in a master-slave configuration. The master laser is an external-cavity laser that operates in a chaotic regime while for the slave laser we consider two configurations. In the first one, the slave laser is also an external-cavity laser, subjected to, its own optical feedback and the optical injection from the master laser. In the second one, the slave laser is subject only to the optical injection from the master laser. Depending on the operating conditions the synchronization between the two lasers, whenever it exists, can be either isochronous or anticipated. We perform a detailed study of the parameter regions in which these synchronization regimes occur and how small variations of parameter yield one or the other type of synchronization or an unsynchronized regime.

DOI: 10.1103/PhysRevE.65.056205

PACS number(s): 05.45.Xt, 42.55.Px, 42.65.Sf

I. INTRODUCTION

The synchronization of chaotic systems is a subject that has attracted a lot of attention in the past ten years. Fujisaka and Yamada [1–3] did early work on the synchronization of the coupled chaotic systems, but it was not until the work of Pecora and Carroll [4] that the subject received full attention from the scientific community. The fact that two chaotic systems can be synchronized was later explored by Cuomo and Oppenheim [5], who built a circuit version of the Lorenz equations and showed the possibility of using this system as a communication scheme to transmit a small speech signal. The signal was hidden in the fluctuations of the x signal of the master circuit. The slave circuit generated its own synchronized x' signal and by subtracting $x - x'$ the speech signal could be recovered. Since then, several schemes for the use of synchronized chaotic systems for secure communication have been proposed [6–10]. Unfortunately, most of the schemes proposed in the literature do not seem to be as secure as expected. Several studies have shown that by using nonlinear dynamics techniques the message can be unmasked [11–15].

The synchronization of chaotic semiconductor lasers has been extensively studied [16–36] since these devices are the key elements of all-optical communication systems. Locquet *et al.* [37] have shown that when the master laser and the slave laser are both external-cavity lasers, two different synchronization regimes might occur. When both lasers have the same amount of optical feedback (and the external-cavity length is the same for both lasers), the slave laser intensity, $I_s(t)$, synchronizes with the intensity injected from the master laser, $I_m(t - \tau_c)$, where τ_c is the flight time from the master laser to the slave laser. When the lasers have the same amount of optical injection (in other words, when the master laser feedback rate is equal to the sum of the slave laser feedback rate and the optical coupling rate), the synchronization of $I_s(t)$ with $I_m(t - \tau_c + \tau)$ occurs, where τ is the external cavity round-trip time (which is the same for both

lasers). Synchronization with a lag time τ_c corresponds to the synchronization of the slave optical field with the injected field (*isochronous synchronization*), while synchronization with a lag time $\tau_c - \tau$ corresponds to the case when the field of the slave laser anticipates the injected field by an anticipation time equal to τ (*anticipated synchronization*).

It has recently been shown that these two types of synchronization exhibit a different robustness with respect to noise, frequency detuning, and they differ in the response of the slave to current modulation of the master laser [38]. Moreover, several authors have demonstrated numerically and experimentally [33,39–41] that the two synchronization regimes can also occur when the slave laser is not subjected to optical feedback.

In this paper we numerically characterize these regimes of synchronization by studying the parameter regions in which they occur. We consider two configurations: in the first one, the slave laser is an external-cavity laser, subjected to its own optical feedback and the optical injection from the master laser (*closed-loop scheme*). In the second one, the slave laser is subjected only to the optical injection from the master laser (*open-loop scheme*). We find that in both configurations the parameter region in which the isochronous synchronization occurs is close to the parameter region in which the stable cw injection-locking occurs. However, an advantage of the closed-loop scheme is that it leads to a better synchronization quality than the open-loop scheme. We also show that the anticipated synchronization occurs in a very tiny parameter region, indicating that it is not an injection-locking-type phenomenon.

When the parameter region in which the anticipated synchronization occurs is close to the parameter region in which the isochronous synchronization occurs, a parameter variation might induce a transition from one regime to the other. In the second part of this paper we study under which conditions this transition is likely to occur, for an open-loop scheme. We find that the two synchronization regions are close to each other when the lasers operate close to threshold. In this case, a transition from the anticipated to the iso-

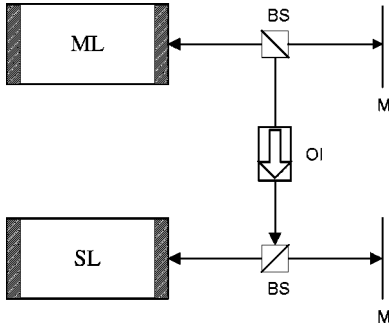


FIG. 1. Schematic representation of the unidirectionally coupled external-cavity lasers. ML is the master laser, SL is the slave laser, OI is the optical isolator, BS is the beam splitter, and M is the mirror.

chronous synchronization occurs when the injection rate is increased or when the parameter variations of the slave laser lead to a decrease of the output power of the solitary slave laser. For all other parameter variations, the synchronization with a lag time $\tau_c - \tau$ is lost and a transition to the other type of synchronization does not occur. On the contrary, when the lasers operate well above threshold, the different regimes of synchronization occur in different ranges of the optical coupling strengths, and a variation of the internal parameters or the coupling strength does not lead to a transition to the other synchronization regime but the lasers usually become unsynchronized.

This paper is organized as follows. Section II presents the model. In Sec. III we describe the different possible synchronized solutions. In Sec. IV we discuss the parameter regions in which the two types of synchronization occur and Sec. V studies the possible transitions between these synchronization regimes. Finally, Sec. VI presents our conclusions.

II. THE MODEL

Figure 1 shows schematically the setup of the system under study. The master laser (ML) and the slave laser (SL) are identical semiconductor lasers with optical feedback from external mirrors. We assume that the mirrors are positioned such that the external-cavity length (defined as the distance between the laser facet and the mirror) is the same for both lasers. The output of the ML is injected into the SL via the optical isolator (OI).

The rate equations for the complex electric fields and the carrier densities in the lasers are the well-known Lang-Kobayashi equations, where the equation for the field in the SL contains an additional term that accounts for the optical injection from the ML. The equations are [31,38,43]

$$\dot{E}_i = \frac{1+i\alpha}{2} [G_i(t) - 1/\tau_{p,i}] E_i(t) + \gamma_i E_i(t-\tau) \exp[-i(\omega\tau)_i] + \eta E_m(t-\tau_c) \exp[-i(\omega_m\tau_c - \Delta\omega t)], \quad (1)$$

$$\dot{N}_i = J_i/e - N_i(t)/\tau_{n,i} - G_i(t)|E_i(t)|^2. \quad (2)$$

Here, the indices $i=m$ and $i=s$ refer to the ML and the SL, respectively, E_i is the slowly varying complex field, and N_i is the normalized carrier number. The equations are written in the reference frame where the complex optical fields of the lasers are given by $E_m \exp(i\omega_m t)$, $E_s \exp(i\omega_s t)$, where ω_m , ω_s are the optical frequencies of the solitary lasers. The term $\eta E_m(t-\tau_c) \exp[-i(\omega_m\tau_c - \Delta\omega t)]$ in Eq. (1) exists only for the SL, and accounts for the light injected from the ML. $\Delta\omega = \omega_m - \omega_s$ is the frequency detuning between the lasers.

The other parameters are as follows: $\tau_{p,i}$ is the photon lifetime, α is the linewidth enhancement factor, $G_i = G_n(N_i - N_0)/(1 + \epsilon|E_i|^2)$ is the optical gain (where G_n is the differential gain, N_0 is the carrier number at transparency, ϵ is the gain saturation coefficient), and $(\omega\tau)_i$ is the phase accumulation after one round trip in the external cavity. J_i is the injection current, e is the electric charge, and $\tau_{n,i}$ is the carrier lifetime. The model does not include multiple reflections in the external cavity, and therefore it is valid for weak feedback levels. Notice that we have assumed that the optical field does not experience any distortion during its propagation from the master to the slave laser. We have also neglected the spontaneous emission noise, which degrades the synchronization quality [25,38]. It has been shown [38] that the anticipated synchronization is much more sensitive to noise than the isochronous synchronization.

To characterize the quality of the synchronization between the output intensities of the lasers we calculate two correlation coefficients,

$$C_1 = \frac{\langle [I_m(t+\tau_1) - \langle I_m \rangle][I_s(t) - \langle I_s \rangle] \rangle}{\{ \langle [I_m(t) - \langle I_m \rangle]^2 \rangle \langle [I_s(t) - \langle I_s \rangle]^2 \rangle \}^{1/2}}, \quad (3)$$

$$C_2 = \frac{\langle [I_m(t+\tau_2) - \langle I_m \rangle][I_s(t) - \langle I_s \rangle] \rangle}{\{ \langle [I_m(t) - \langle I_m \rangle]^2 \rangle \langle [I_s(t) - \langle I_s \rangle]^2 \rangle \}^{1/2}}, \quad (4)$$

where $\tau_1 = -\tau_c$ and $\tau_2 = \tau - \tau_c$. The regime of the isochronous synchronization with a lag time τ_c is characterized by a large value of C_1 , while the regime of the anticipated synchronization with a lag time $\tau_c - \tau$ is characterized by a large value of C_2 .

III. TIME LAGGED SYNCHRONOUS SOLUTIONS

If there is no frequency detuning ($\omega_m = \omega_s = \omega$) Eqs. (1) and (2) can be rewritten as

$$\dot{I}_m(t) = [G_m(t) - 1/\tau_{p,m}] I_m(t) + 2\gamma_m \sqrt{I_m(t-\tau)I_m(t)} \cos \xi_m(t, \tau), \quad (5)$$

$$\dot{\psi}_m(t) = \frac{\alpha}{2} [G_m(t) - 1/\tau_{p,m}] - \gamma_m \sqrt{\frac{I_m(t-\tau)}{I_m(t)}} \sin \xi_m(t, \tau), \quad (6)$$

$$\dot{N}_m(t) = J_m/e - N_m(t)/\tau_{n,m} - G_m(t)I_m(t), \quad (7)$$

$$\begin{aligned} \dot{I}_s(t) = & [G_s(t) - 1/\tau_{p,s}]I_s(t) + 2\gamma_s\sqrt{I_s(t-\tau)I_s(t)}\cos\xi_s(t,\tau) \\ & + 2\eta\sqrt{I_m(t-\tau_c)I_s(t)}\cos\xi_{ms}(t,\tau_c), \end{aligned} \quad (8)$$

$$\begin{aligned} \dot{\psi}_s(t) = & \frac{\alpha}{2}[G_s(t) - 1/\tau_{p,s}] - \gamma_s\sqrt{\frac{I_s(t-\tau)}{I_s(t)}}\sin\xi_s(t,\tau) \\ & - \eta\sqrt{\frac{I_m(t-\tau_c)}{I_s(t)}}\sin\xi_{ms}(t,\tau_c), \end{aligned} \quad (9)$$

$$\dot{N}_s(t) = J_s/e - N_s(t)/\tau_{n,s} - G_s(t)I_s(t), \quad (10)$$

where I_m , ψ_m , I_s , and ψ_s are the intensity and the phase of the master and the slave lasers ($E_m = \sqrt{I_m}e^{i\psi_m}$, $E_s = \sqrt{I_s}e^{i\psi_s}$), and $\xi_m(t,\tau) = \psi_m(t) - \psi_m(t-\tau) + \omega\tau$, $\xi_s(t,\tau) = \psi_s(t) - \psi_s(t-\tau) + \omega\tau$, $\xi_{ms}(t,\tau_c) = \psi_s(t) - \psi_m(t-\tau_c) + \omega\tau_c$. Two cases are interesting to analyze.

(1) *Anticipated synchronization.* If the operating conditions and the internal parameters of the lasers are identical, and the feedback levels of the master and the slave lasers are related by the condition $\gamma_m = \gamma_s + \eta$, the equations for the slave laser can be rewritten as

$$\begin{aligned} \dot{I}_s(t) = & [G_s(t) - 1/\tau_{p,m}]I_s(t) + 2\gamma_m\sqrt{I_s(t-\tau)I_s(t)}\cos\xi_s(t,\tau) \\ & + 2\eta[\sqrt{I_m(t-\tau_c)I_s(t)}\cos\xi_{ms}(t,\tau_c) \\ & - \sqrt{I_s(t-\tau)I_s(t)}\cos\xi_s(t,\tau)], \end{aligned} \quad (11)$$

$$\begin{aligned} \dot{\psi}_s(t) = & \frac{\alpha}{2}[G_s(t) - 1/\tau_{p,m}] - \gamma_m\sqrt{\frac{I_s(t-\tau)}{I_s(t)}}\sin\xi_s(t,\tau) \\ & - \eta\left[\sqrt{\frac{I_m(t-\tau_c)}{I_s(t)}}\sin\xi_{ms}(t,\tau_c) \right. \\ & \left. - \sqrt{\frac{I_s(t-\tau)}{I_s(t)}}\sin\xi_s(t,\tau)\right], \end{aligned} \quad (12)$$

$$\dot{N}_s(t) = J_m/e - N_s(t)/\tau_{n,m} - G_s(t)I_s(t). \quad (13)$$

Comparing Eqs. (11)–(13) with Eqs. (5)–(7) it is clear that the synchronization manifold is

$$I_s(t-\tau) = I_m(t-\tau_c), \quad (14)$$

$$\xi_s(t,\tau) = \xi_{ms}(t,\tau_c), \quad (15)$$

$$N_s(t-\tau) = N_m(t-\tau_c). \quad (16)$$

Equation (15) implies that the phases of the slowly varying fields are related by

$$\psi_s(t-\tau) - \omega\tau = \psi_m(t-\tau_c) - \omega\tau_c \quad (17)$$

and therefore that the optical fields are equal but lagged in time. This corresponds to the complete (or identical) synchronization of the coupled systems, with a lag time $\tau_c - \tau$. In the expression of the time lag, the term τ_c is due to the propagation time of light between the two lasers, while the term τ is due to the fact that the master is a time-delayed

system [31,44]. When $\tau_c < \tau$, the optical field of the slave laser at time t anticipates the optical field of the master laser at time t [31]; otherwise it lags behind. The lag time $\tau_c - \tau$ is typical of unidirectionally coupled time-delayed systems and has been observed numerically in the coupled semiconductor lasers subject to an incoherent optical feedback and injection [36] and experimentally in the semiconductor lasers subject to a delayed optoelectronic feedback [45].

(2) *Isochronous synchronization.* If the lasers have the same operating conditions, equal feedback levels ($\gamma_m = \gamma_s$), equal internal parameters but different cavity decays (such that $1/\tau_{p,s} = 1/\tau_{p,m} + 2\eta/\sqrt{1+\alpha^2}$), the equations for the slave laser can be rewritten as

$$\begin{aligned} \dot{I}_s(t) = & [G_s(t) - 1/\tau_{p,m}]I_s(t) + 2\gamma_m\sqrt{I_s(t-\tau)I_s(t)}\cos\xi_s(t,\tau) \\ & + 2\eta[\sqrt{I_m(t-\tau_c)I_s(t)}\cos\xi_{ms}(t,\tau_c) \\ & - I_s(t)/\sqrt{1+\alpha^2}], \end{aligned} \quad (18)$$

$$\begin{aligned} \dot{\psi}_s(t) = & \frac{\alpha}{2}[G_s(t) - 1/\tau_{p,m}] - \gamma_m\sqrt{\frac{I_s(t-\tau)}{I_s(t)}}\sin\xi_s(t,\tau) \\ & - \eta\left[\sqrt{\frac{I_m(t-\tau_c)}{I_s(t)}}\sin\xi_{ms}(t,\tau_c) + \alpha/\sqrt{1+\alpha^2}\right], \end{aligned} \quad (19)$$

$$\dot{N}_s(t) = J_m/e - N_s(t)/\tau_{n,m} - G_s(t)I_s(t). \quad (20)$$

Comparing Eqs. (18)–(20) with Eqs. (5)–(7) it is clear that the synchronization manifold is

$$I_s(t) = I_m(t-\tau_c), \quad (21)$$

$$\tan\xi_{ms}(t,\tau_c) = -\alpha, \quad (22)$$

$$N_s(t) = N_m(t-\tau_c), \quad (23)$$

which implies that the phases of the slowly varying fields are related by

$$\tan[\psi_s(t) - \psi_m(t-\tau_c) + \omega\tau_c] = -\alpha. \quad (24)$$

In this case the slave laser synchronizes with the injected field, and due to the finite speed of propagation, the slave laser always lags in time behind the master laser.

Notice that in case (1) the lasers are subjected to different amount of optical feedback, while in case (2) the lasers are subjected to the same amount of optical feedback. As shown in Ref. [42], case (2) is a particular case of a more general situation. If the lasers are subjected to the same feedback level and the cavity losses differ such that $1/\tau_{p,s} = 1/\tau_{p,m} + \delta$ with δ arbitrary, a type of synchronized solution might exist in which

$$I_s(t) = aI_m(t-\tau_c), \quad (25)$$

$$N_s(t) = N_m(t-\tau_c) + \Delta_N, \quad (26)$$

where a and Δ_N are constants. The existence of such solution was analytically demonstrated, under certain approximations, in Ref. [42]. This solution exists even if $\delta=0$, since in this case the carrier difference Δ_N plays a role similar to δ , and if there is a detuning between the optical frequencies of the lasers. Since there is a functional relation between the states of the master and slave systems, this corresponds to a generalized synchronization [46] of the coupled systems, with a lag time τ_c .

Next we consider the case in which the slave laser is a solitary laser, subjected only to the optical injection from the master laser (open-loop scheme). In this case, when the injection rate is equal to the master feedback rate ($\eta=\gamma_m$) a synchronized solution with a lag time $\tau_c-\tau$ exists. This synchronized solution is simply a special case of solution (14)–(16) when the slave is not subjected to feedback ($\gamma_s=0$). Several authors [33,39–41] have found that it is also possible to obtain a certain degree of synchronization with a lag time τ_c with an open-loop scheme. However, with an open-loop scheme a chaotic synchronized solution with a lag time τ_c does not exist, because in case (2) the lasers must be subjected to the same feedback level. Koryukin and Mandel have shown [39] that, in the special case $\eta=\gamma_m$, a perfectly synchronized solution with a lag time τ_c exists if the amplitude and the phase of the slowly varying optical field are periodic, with a period τ/N , where N is a positive integer.

IV. SYNCHRONIZATION REGIONS

We simulate Eqs. (1) and (2) with the parameters $\tau=1$ ns, $\tau_p=2$ ps, $\tau_n=2$ ns, $\alpha=5$, $G_n=1.5\times 10^4$ s $^{-1}$, $N_0=1.5\times 10^8$, $\epsilon=5\times 10^{-7}$, $\omega\tau=0$ rad. We assume for the moment that the internal parameters are identical for the two lasers.

First, we characterize the synchronization regions in the parameter space (frequency detuning, injection rate). The synchronization regions strongly depend on the chaotic behavior of the master laser, which in turn is determined by the injection current and the feedback level. Let us consider a situation in which the lasers operate well above threshold ($J_m=J_s=1.85J_{th}$, where $J_{th}=14.7$ mA is the threshold current of the solitary laser) and the master laser is subjected to moderated optical feedback ($\gamma_m=10$ ns $^{-1}$, which is within the limits of validity of the model since we find qualitatively similar results when two or three external reflections are taken into account). For these parameters the master laser is in the so-called coherence collapse (CC) regime, characterized by fast, chaotic intensity fluctuations (see Fig. 2).

In Fig. 3(a) we show the synchronization region when the lasers are subject to the same feedback level ($\gamma_s=\gamma_m=10$ ns $^{-1}$). The horizontal axis is the frequency detuning between the lasers, the vertical axis is the optical injection rate, and the gray levels represent the value of C_1 (the dark gray levels represent large correlation). The synchronization region is broad, allowing for frequency detunings up to tens of gigahertz, and is asymmetric. Figure 3(b) displays the same correlation coefficient as Fig. 3(a) (and for the same parameter values), but when the slave laser is subjected to cw optical injection. As was reported in Ref. [42] for the case

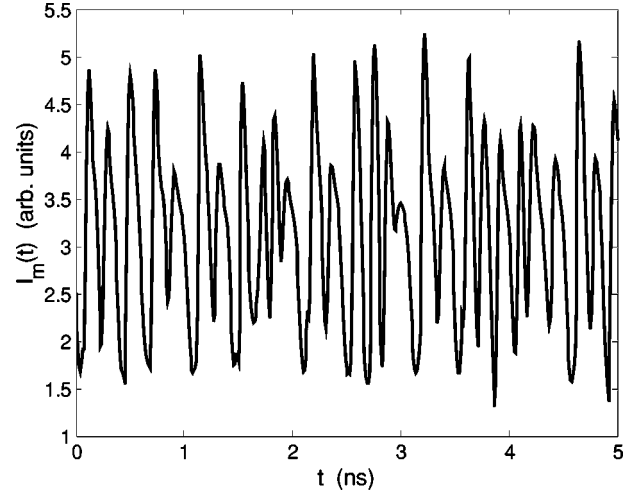


FIG. 2. Intensity fluctuations of the ML operating on the coherence collapse regime. $\gamma_m=10$ ns $^{-1}$, $J_m=1.85J_{th}=27.2$ mA.

of an open-loop scheme, we find that the shapes of the chaotic synchronization region [in Fig. 3(a)] and the cw injection-locking region [in Fig. 3(b)] are similar. We can see that the chaotic synchronization region is broader than the cw injection-locking region. The similarity of the two regions suggests that isochronous synchronization is an injection-locking-type phenomenon.

Figures 4(a) and 4(b) show the same as Figs. 3(a) and 3(b) but in the case of an open-loop scheme ($\gamma_s=0$). Again we observe that there is a similarity between the chaotic synchronization region in Fig. 4(a) and the cw injection-locking region in Fig. 4(b). We can also notice that, for low injection levels, the correlation coefficient is larger for cw injection-locking than for chaotic synchronization.

Comparing Figs. 3(a) and 4(a) (which are done with the same gray scale), it is clear that the synchronization quality is in general lower when the slave laser does not have its own feedback. For example, for zero frequency detuning and for the maximum injection rate considered in Figs. 3(a) and 4(a) ($\eta=50$ ns $^{-1}$), $C_1=0.999$ for a close-loop scheme while $C_1=0.86$ for an open-loop scheme. Moreover, in order to obtain a correlation coefficient of 0.99 with an open-loop scheme, the injection rate has to be increased to as much as 170 ns $^{-1}$ for our parameter values. The lower degree of correlation is a disadvantage when comparing open- and close-loop schemes. Since the coupling strength has a maximum value in a real experiment, it will not always be possible to achieve a good degree of synchronization with an open-loop scheme. Similar results were experimentally obtained in Ref. [40]: the injected power had to be about one hundred times larger than the power fed back into the master laser cavity in order to observe good synchronization with an open-loop scheme.

The difference in synchronization quality for the cases of a slave laser with or without feedback at a lag time τ_c can be explained by the fact that when $\gamma_m=\gamma_s$, an analytical synchronized solution exists [Eqs. (25)–(26)]. On the contrary, as discussed in the preceding section, when $\gamma_s=0$ no such solution exists. Therefore, in the case of an open-loop

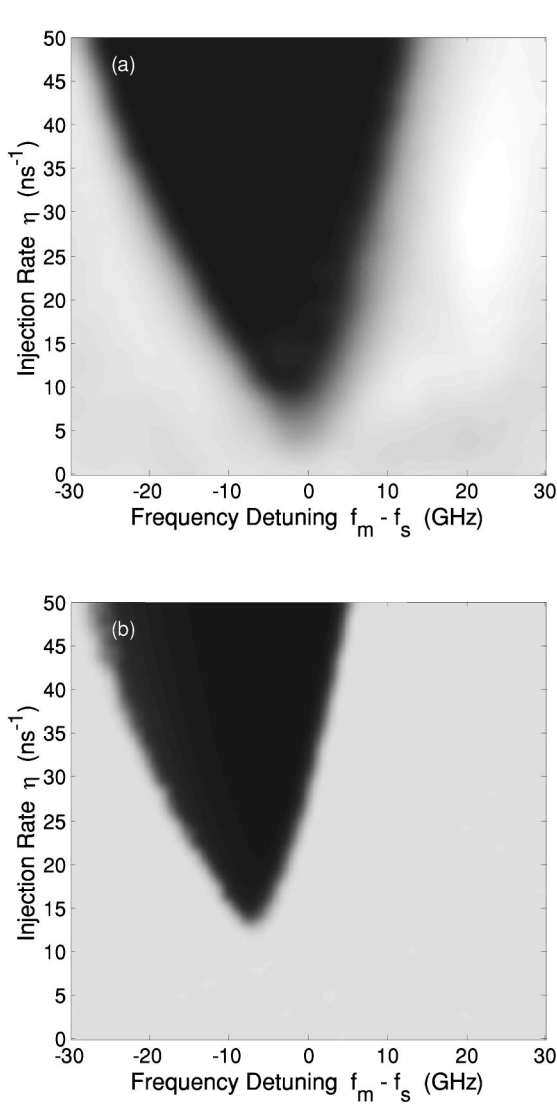


FIG. 3. (a) Correlation coefficient C_1 as a function of the frequency detuning and the optical coupling strength, when the slave is an external cavity laser subjected to chaotic injection from the master laser. $\gamma_m = \gamma_s = 10 \text{ ns}^{-1}$. (b) Correlation coefficient C_1 as a function of the frequency detuning and the optical coupling strength, when the slave is an external cavity laser subjected to cw injection from the master laser. $\gamma_s = 10 \text{ ns}^{-1}$. All other parameters as in Fig. 2.

scheme, the chaotic synchronization with a lag time τ_c corresponds to a direct generalization of cw injection locking, whereas in the case of a close-loop scheme there is a “true” synchronization in the sense that a synchronized solution exists. As a consequence, the synchronization with a close-loop scheme has advantages for applications where a high degree of synchronization is required. However, it has the disadvantage that additional components have to be used in the experimental setup. In particular, it can be easily shown that in order for an isochronous solution to exist, the external mirror at the slave laser has to be very carefully positioned such that the phase accumulations in the external cavities verify $(\omega\tau)_m - (\omega\tau)_s = \Delta_\phi$, where Δ_ϕ is a constant. In the special case of zero frequency detuning, and in the reference frame

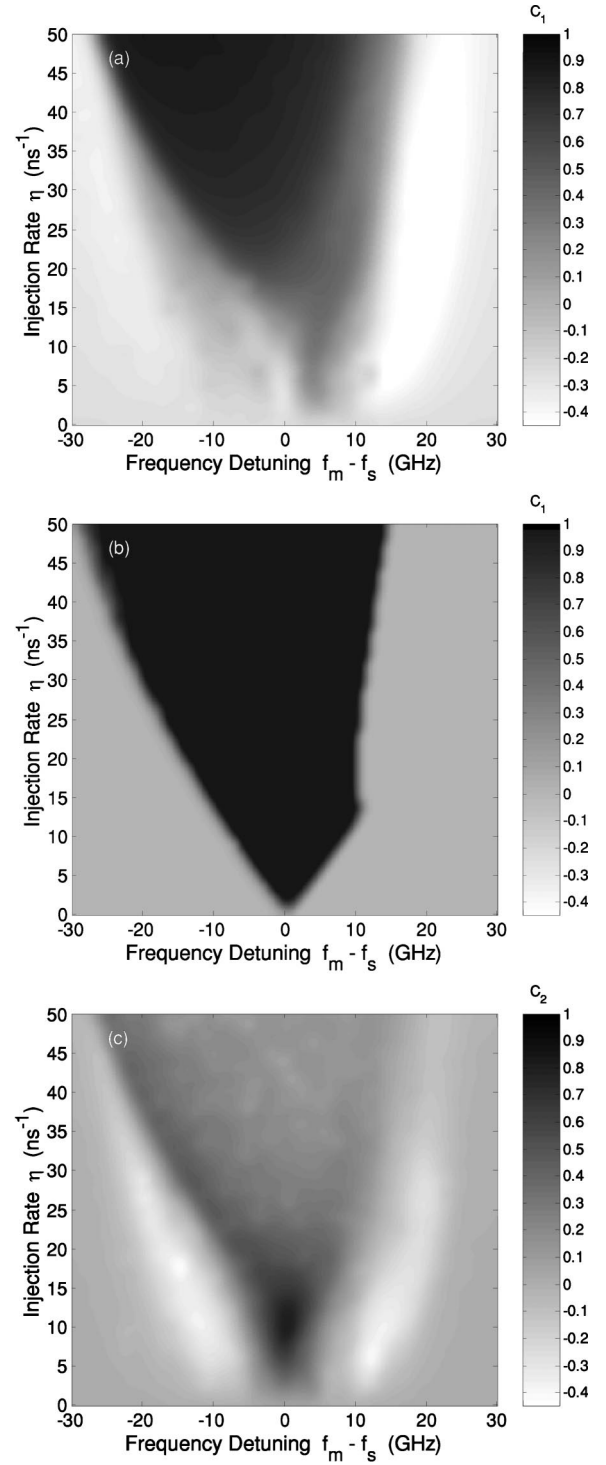


FIG. 4. (a) Correlation coefficient C_1 as a function of the frequency detuning and the optical coupling strength, when the slave laser is subjected only to chaotic injection from the master laser. $\gamma_m = 10 \text{ ns}^{-1}$, $\gamma_s = 0$. (b) Correlation coefficient C_1 as a function of the frequency detuning and the optical coupling strength, when the slave laser is subjected only to cw injection from the master laser. $\gamma_s = 0 \text{ ns}^{-1}$. (c) Correlation coefficient C_2 as a function of the frequency detuning and the optical coupling strength, when the slave laser is subjected only to chaotic injection from the master laser. All other parameters as in Fig. 2.

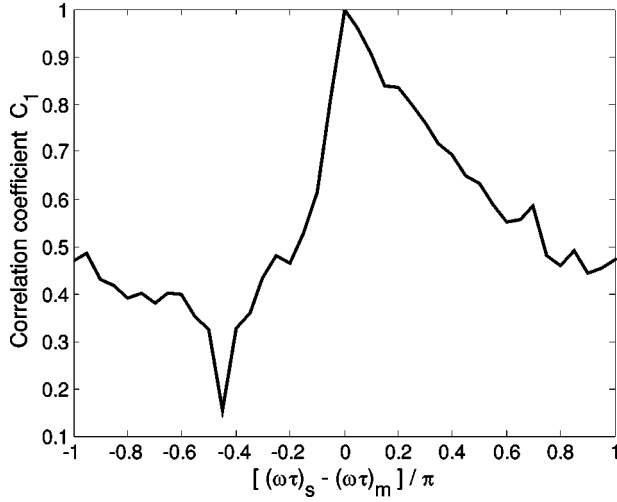


FIG. 5. Correlation coefficient C_1 as a function of the difference between the phase accumulations in the external cavities of the slave laser, $(\omega\tau)_s$, and of the master laser, $(\omega\tau)_m$. $\Delta\omega=0$, $\eta=25 \text{ ns}^{-1}$, all other parameters as in Fig. 2.

we use, $\Delta\phi=0$. This fact is shown in Fig. 5, where we assume that the lasers have identical frequencies but slightly different delay times. Small differences in the delay times lead to significant differences in the phase accumulations and to a strong degradation of the synchronization quality.

Since in the case of an open-loop scheme synchronization with a lag time $\tau_c - \tau$ is possible when $\eta = \gamma_m$ and $\Delta\omega=0$, it is also interesting to study the value of C_2 , defined in Eq. (4), in the parameter space (detuning, injection rate). This is displayed in Fig. 4(c), which shows C_2 on the same gray scale as Figs. 3(a) and 4(a). Comparing Figs. 4(a) and 4(c) it is clear that the correlation coefficient C_1 calculated with a lag time τ_c is usually larger than the correlation coefficient C_2 calculated with a lag time $\tau_c - \tau$. However, when $\eta \sim \gamma_m$ and for small detuning, $C_2 > C_1$. This is because when $\eta = \gamma_m$ and $\Delta\omega=0$ an analytic solution exists for synchronization with a lag time $\tau_c - \tau$, as discussed in the preceding section. We obtain a reasonable quality of synchronization for frequency detunings up to a few gigahertz. Notice that in the two white regions in Fig. 4(c) a certain degree of antisynchronization occurs since the correlation coefficient is negative (however, the dynamics is not anticorrelated since in these regions C_2 is at most -0.4).

Figure 6 shows the value of C_2 when the slave laser is an external-cavity laser and its feedback level is varied such that $\gamma_s = \gamma_m - \eta$. As mentioned before, this is a necessary condition for the existence of a perfectly synchronized solution with a lag time $\tau_c - \tau$, in the absence of frequency detuning. Since γ_s cannot be negative, we are restricted in Fig. 6 to a maximum value of the injection rate η , which is the feedback rate of the master laser, $\gamma_m = 10 \text{ ns}^{-1}$. It can be seen that even when there is no frequency detuning (in this case a perfectly synchronized solution exists) synchronization does not occur for small injection rates. This means that the synchronized solution is stable only for large enough injection rates (and hence small enough slave feedback rates). Moreover, contrary to isochronous synchronization, a reasonably

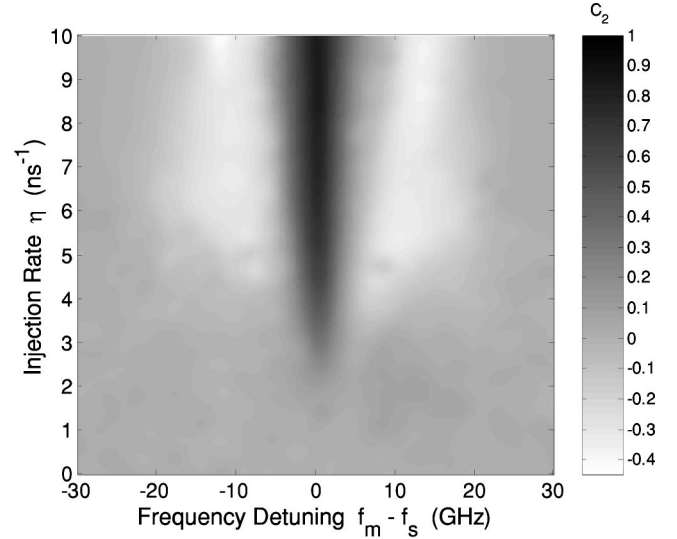


FIG. 6. Correlation coefficient C_2 as a function of the frequency detuning and the optical coupling strength, when $\gamma_s = \gamma_m - \eta$. All other parameters as in Fig. 4.

good level of synchronization is preserved for detunings of only few gigahertz.

From the mathematical point of view the phase space of the master laser is infinite dimensional because of the delayed feedback. Therefore theoretically the maximum value of the dimension of the attractor is infinite. This property of potentially very high dimensional attractors makes delay systems interesting for chaotic secure communications since it has been suggested that high-dimensional dynamics leads to higher security levels [20,21]. It is well accepted that the dimension of the chaotic attractor associated with the master laser dynamics increases with the feedback rate γ_m (and with the delay time τ). It is therefore interesting to determine how the synchronization quality evolves when the master feedback rate is changed, and how the minimum injection rate above which the synchronization occurs depends on the master feedback rate.

Figure 7 displays the synchronization regions in the parameter space (master feedback rate, injection rate) when there is no frequency detuning. In Fig. 7(a) $\gamma_s = \gamma_m$, in Fig. 7(b) $\gamma_s = 0$, and in Fig. 7(c) $\gamma_s = \gamma_m - \eta$. Since γ_s cannot be negative, in Fig. 7(c) the maximum value of η is γ_m . As in the previous figures, Figs. 7(a) and 7(b) display the value of C_1 , while Fig. 7(c) displays the value of C_2 . It can be clearly seen that when γ_m increases, the injection rate has to be increased in order to maintain the synchronization quality. For example, when $\gamma_s = \gamma_m$ a correlation coefficient $C_1 > 0.999$ can be obtained for an injection rate $\eta > 20 \text{ ns}^{-1}$ for $\gamma_m = 10 \text{ ns}^{-1}$, while $\eta > 45 \text{ ns}^{-1}$ for $\gamma_m = 20 \text{ ns}^{-1}$. In the case of an open-loop scheme, an injection rate as high as 100 ns^{-1} leads to a correlation coefficient $C_1 = 0.95$ when $\gamma_m = 10 \text{ ns}^{-1}$ and $C_1 = 0.79$ when $\gamma_m = 20 \text{ ns}^{-1}$. Since in experiments the injection rate has a maximum value, it can be expected that there is a maximum value of the master feedback rate above which high-quality synchronization with an open-loop scheme is not possible. Figure 7(c) shows that in the case of anticipated synchronization there is also the

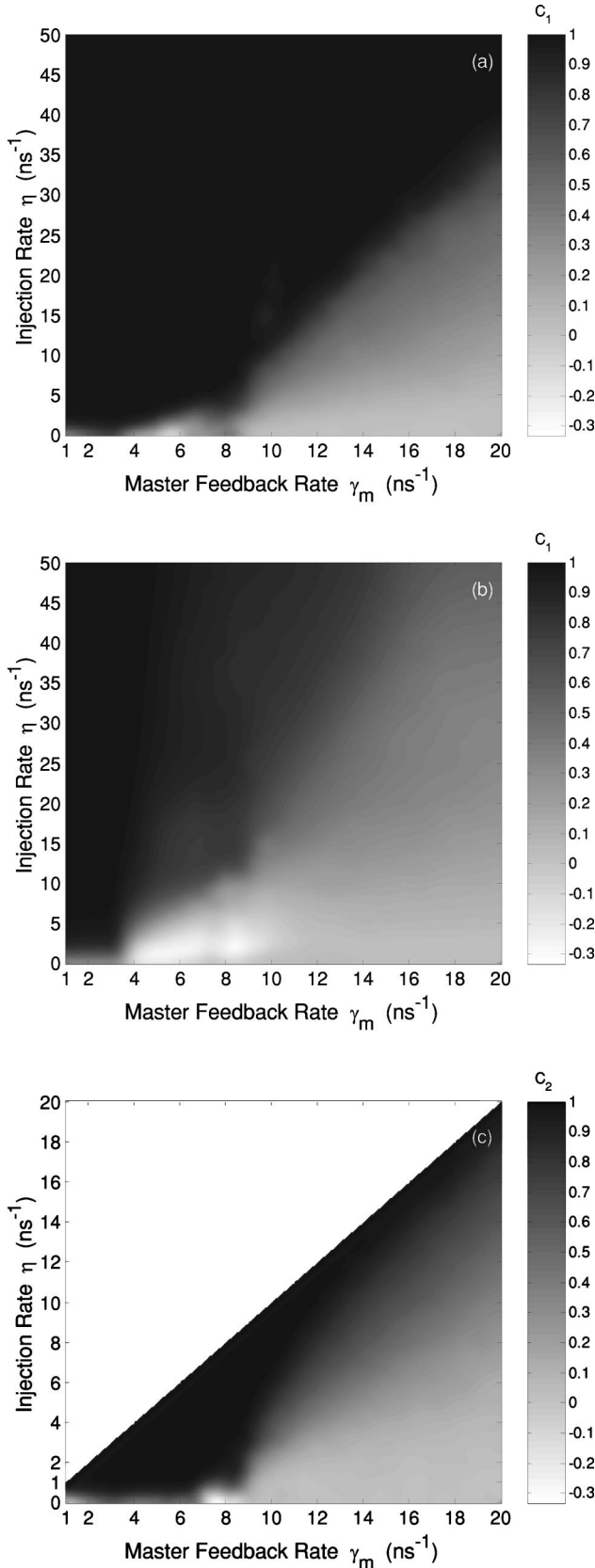


FIG. 7. Synchronization regions in the parameter space (master feedback rate, optical coupling rate). (a) $\gamma_s = \gamma_m$, the value of C_1 is plotted. (b) $\gamma_s = 0$, the value of C_1 is plotted. (c) $\gamma_s = \gamma_m - \eta$, the value of C_2 is plotted. $\Delta\omega = 0$, all other parameters as in Fig. 4.

need to increase the injection rate when the master feedback rate is increased. Moreover, one can notice that the larger the value of the feedback rate γ_m , the closer η must be to γ_m in order to ensure good synchronization.

V. TRANSITIONS BETWEEN SYNCHRONIZATION REGIMES

As we have seen, with an open-loop scheme it is possible to observe synchronization with a lag time $\tau_c - \tau$ (if $\eta = \gamma_m$), and also synchronization with a lag time τ_c . Therefore, it might be that under adequate conditions the two regimes coexist (i.e., they occur for identical or close parameter values).

Koryukin and Mandel [39] have recently shown that a transition from synchronization with a lag time $\tau_c - \tau$ to synchronization with a lag time τ_c occurs when the injection rate η is slightly *increased* above γ_m or when the injection current J_s is slightly *decreased* below J_m . The parameters considered in Ref. [39] correspond to a master laser operating in the so-called low-frequency fluctuations (LFF) regime. This regime occurs when the laser is biased close to the threshold and subjected to weak to moderate feedback, and is characterized by abrupt, random, intensity dropouts followed by deterministic, steplike recoveries.

In this section we analyze the possible transitions from one regime of synchronization to the other, in the case of an open-loop scheme, and considering an injection current close to threshold (such that the master laser operates in the LFF regime). Figures 8(a) and 8(b) display the correlation coefficients C_1 and C_2 , respectively, in the parameter space (frequency detuning, injection rate). All other parameters are the same as in Figs. 4(a), and 4(c) except that the injection current is lower ($J_m = J_s = 1.02J_{th}$).

When comparing Fig. 8(a) with Fig. 4(a), it is clear that for lower current the synchronization region with a lag time τ_c *shifts down* towards lower values of η . As could be expected, Fig. 8(b) shows that anticipated synchronization occurs when η is close to γ_m and the frequency detuning is small. Since the threshold injection rate for synchronization with a time lag τ_c now is slightly larger than γ_m ($= 10 \text{ ns}^{-1}$), and the injection rate for synchronization with a lag time $\tau_c - \tau$ is still η equal or close to γ_m , a small increase of η above $\eta = \gamma_m$ will cause a transition from synchronization with a lag time $\tau_c - \tau$ to synchronization with a time lag τ_c . This is in agreement with the observations of Ref. [39].

This transition is illustrated in Fig. 9, which shows the master laser and slave laser intensities, averaged in time to simulate the typical bandwidth of the detectors used in experiments. Figure 9(a) displays $I_m(t - \tau_c)$ for a feedback level $\gamma_m = 10 \text{ ns}^{-1}$, while Figs. 9(b), 9(c), and 9(d) display $I_s(t)$ for different injection rates. Notice that in Fig. 9(a) I_m is lagged τ_c in time. For $\eta = \gamma_m = 10 \text{ ns}^{-1}$ [Fig. 9(b)] $I_s(t)$ is identical to $I_m(t - \tau_c + \tau)$, therefore $I_s(t)$ anticipates the injected intensity $I_m(t - \tau_c)$ by an anticipation time τ ($= 1 \text{ ns}$). If η is increased to 12 ns^{-1} [Fig. 9(c)] we observe a transition to synchronization with a lag time τ_c . Notice that the time traces shown in Figs. 9(a) and 9(c) are most of the

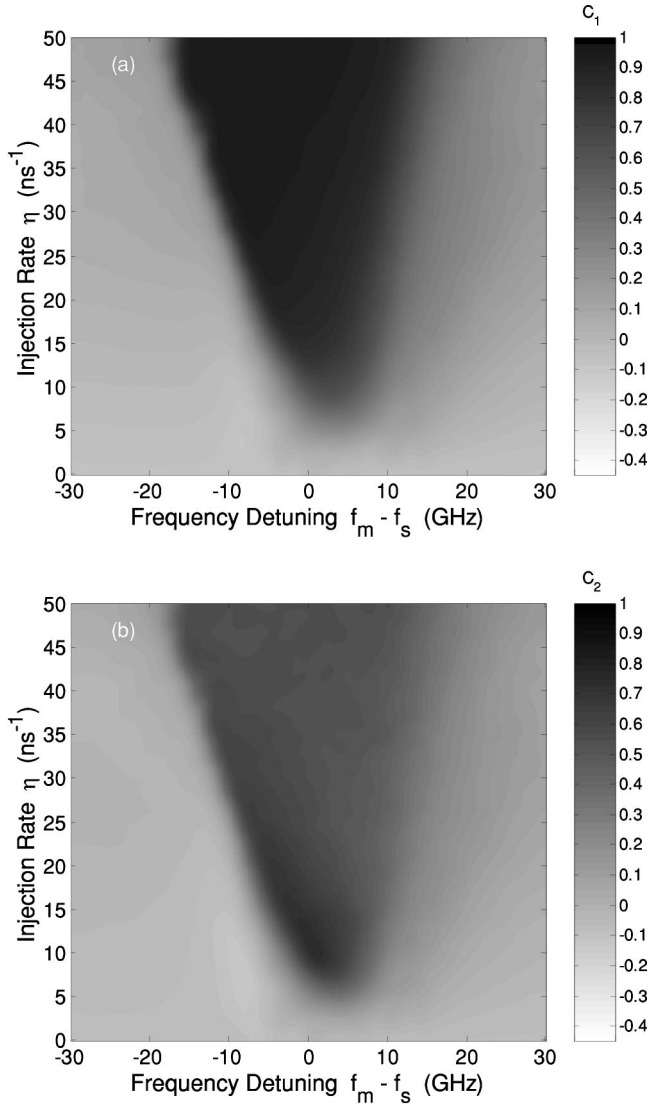


FIG. 8. Correlation coefficients C_1 (a), C_2 (b) as a function of the frequency detuning and the optical coupling strength. $\gamma_m = 10 \text{ ns}^{-1}$, $\gamma_s = 0$, $J_m = J_s = 1.02 J_{th} = 15 \text{ mA}$. All other parameters as in Fig. 4.

time equal, the main difference being a less pronounced drop out in the intensity of the slave laser. On the other hand, when η is decreased to 9 ns^{-1} [Fig. 9(d)] synchronization with a lag time $\tau_c - \tau$ disappears (because the condition $\eta = \gamma_m$ is not met any more), and a transition to synchronization with a lag time τ_c does not occur (because the system is driven outside of the synchronization region). Notice that the time traces shown in Figs. 9(a) and 9(d) are completely different.

We also observe that, as previously reported in Ref. [39], when the injection current in the slave laser J_s is slightly decreased a transition to the isochronous synchronization occurs, however, this transition does not happen if J_s is increased. In addition, we find that the transition occurs when the slave laser photon lifetime, $\tau_{p,s}$ or the carrier lifetime $\tau_{n,s}$ are *decreased* and when the slave carrier number at transparency $N_{0,s}$ is *increased*. The parameter changes that lead to a

transition to synchronization with a lag time τ_c always correspond to a *decrease* of the solitary slave laser output power, I_s^{sol} . We have checked the generality of the above conclusion, by doing several parameter variations that compensated one another. It is remarkable that an increase of the injection rate (which causes a transition to synchronization with a lag time τ_c) and a decrease of the solitary slave laser power, I_s^{sol} , both correspond to an increase of the ratio between the injected power and the solitary slave power. A certain level of adequate parameter mismatch is needed to induce a transition between the synchronization regions, but if the mismatches become too large, synchronization is lost. This is due to the fact that when the mismatch is too large, the chaotic attractors of the master and the slave systems become too different to allow synchronized chaotic orbits [24]. We find that when $\tau_{p,s}$, $\tau_{n,s}$, J_s are increased (all these changes yield an increase of I_s^{sol}), neither type of synchronization occurs. However, if the injection rate η is also increased (above γ_m), we find again the isochronous synchronization. Therefore, synchronization with a lag time $\tau_c - \tau$ only occurs for almost identical parameters while small parameter mismatches either induce a transition to the isochronous synchronization or destroy the synchronization. Since in an experimental setup the lasers will not have exactly identical parameters, our results suggest that it will be more likely to observe experimentally LFF synchronization with a lag time τ_c than with a lag $\tau_c - \tau$ where perfectly matched lasers and a strict observation of the synchronization condition $\eta = \gamma_m$ are needed.

Figure 10 shows as an example of these behaviors, the transitions that occur when a mismatch on τ_n is considered. Figure 10(a) displays the time-averaged master laser intensity, $I_m(t - \tau_c)$ for a feedback level $\gamma_m = 10 \text{ ns}^{-1}$ and a carrier lifetime $\tau_{n,m} = 2 \text{ ns}$, while Figs. 10(b), 10(c), 10(d), and 10(e) display the slave laser time-averaged intensity, $I_s(t)$ for different injection rates and carrier lifetimes $\tau_{n,s}$. When $\tau_{n,s} = \tau_{n,m} = 2 \text{ ns}$ [Fig. 10(b)], complete synchronization of $I_s(t)$ with $I_m(t - \tau_c)$ occurs with a lag time τ . When $\tau_{n,s} = 1.99 \text{ ns}$, $I_s(t)$ [Fig. 10(c)] synchronizes with $I_m(t - \tau_c)$ [Fig. 10(a)] (notice that the dropouts occur nearly simultaneously, but the dropouts of the slave laser intensity are less pronounced). When $\tau_{n,s}$ is increased to 2.01 ns , Fig. 10(d) confirms that none of the two synchronization regimes occur. In Fig. 10(d) $\tau_{n,s} > \tau_{n,m}$ and $\eta = \gamma_m$, however, if η is increased to 12 ns^{-1} , synchronization of $I_s(t)$ [Fig. 10(e)] with $I_m(t - \tau_c)$ [Fig. 10(a)] occurs.

Figure 11 represents the correlation coefficient, $C(\tau^*)$, between the time-averaged $I_s(t)$ and $I_m(t - \tau_c + \tau^*)$, as a function of the variable τ^* , for the four cases considered above. When $\eta = \gamma_m = 10 \text{ ns}^{-1}$ and $\tau_{n,s} = \tau_{n,m} = 2 \text{ ns}$, the correlation coefficient exhibits a global maximum at $\tau^* = \tau$ [Fig. 11(a)], while for $\tau_{n,s} = 1.99 \text{ ns}$ there is a very pronounced maximum located at $\tau^* = 0$ [Fig. 11(b)]. When $\eta = \gamma_m$, $\tau_{n,s} = 2.01 \text{ ns}$ there is a much less pronounced maximum located at $\tau^* = \tau$ [Fig. 11(c)]. In this case, neither type of synchronization occurs but there will still be a tendency to synchronization with a lag time $\tau_c - \tau$ during short intervals of time, explaining the maximum at $\tau^* = \tau$. If $\tau_{n,s}$ is further

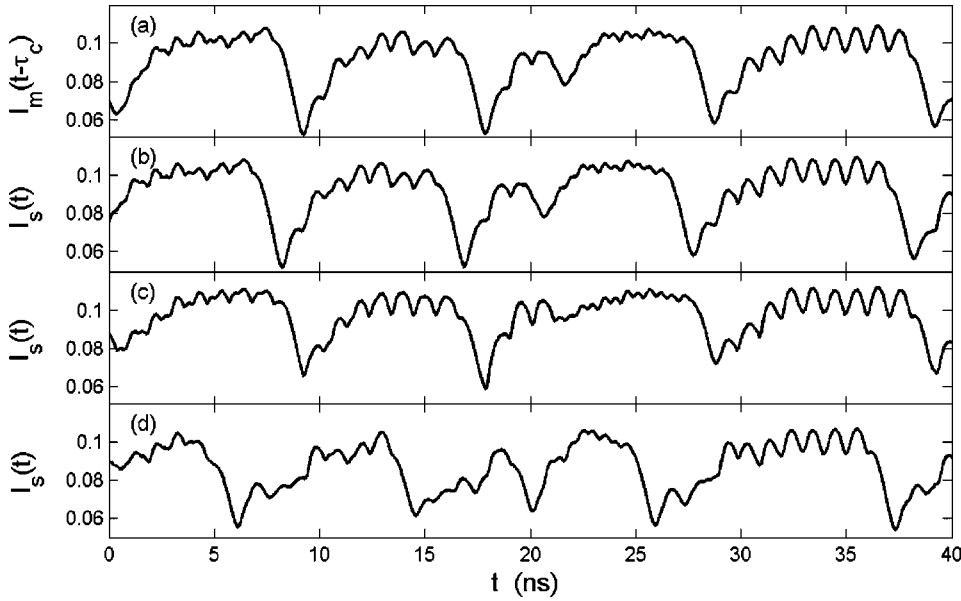


FIG. 9. Time traces of the time-averaged intensities. (a) Intensity of the master laser (lagged τ_c in time) for $\gamma_m = 10 \text{ ns}^{-1}$. Intensity of the slave laser for (b) $\eta = \gamma_m$; (c) $\eta = 12 \text{ ns}^{-1}$; (d) $\eta = 9 \text{ ns}^{-1}$. $\Delta\omega = 0$, all other parameters as in Fig. 4.

increased above $\tau_{n,m}$, this tendency is completed lost. Finally, when η is increased up to 13 ns^{-1} , maintaining $\gamma_m = 10 \text{ ns}^{-1}$, an increase of $\tau_{n,s}$ to 2.01 ns again a maximum located at zero is obtained. These results show that the function $C(\tau^*)$ can be a useful tool for analyzing the synchronization regimes of coupled chaotic systems, and is also a good quantification of the synchronization error [23].

In this section we have identified which parameter changes induce transitions between the two synchronization regimes, extending the results of Koryukin and Mandel [39]. As we have mentioned previously, numerical [40] and experimental [41] studies indicate that while synchronization with a lag time $\tau_c - \tau$ effectively occurs when $\eta = \gamma_m$, the injection rate η must be much larger than γ_m in order to have synchronization with a lag time τ_c . For example, the experimental results of Ref. [40] show that, in order to observe synchronization with a lag time τ_c , the power that is optically injected into the slave laser must be at least one hun-

dred times larger than the power that is fed back into the master laser. Since the authors of Refs. [40] and [41] find that that the two types of synchronization correspond to very different values of the injection rate, small injection rate or parameter changes cannot lead to transitions between the two types of synchronization.

This seems to contradict the results presented in this section. However, it is important to notice that the dynamical regimes considered are different. In this section we considered a master laser operating in the the LFF regime, while in Refs. [40,41] the authors consider a master laser operating in the CC regime (as we have done in the preceding section). In order to clearly show how the synchronization regions depend on the injected current, Fig. 12 displays the synchronization regions in the parameter space (injection current, injection rate). We consider an open-loop scheme, C_1 is represented in Fig. 12(a) and C_2 in Fig. 12(b). The white line displayed in Fig. 12(a) corresponds to the injection rate

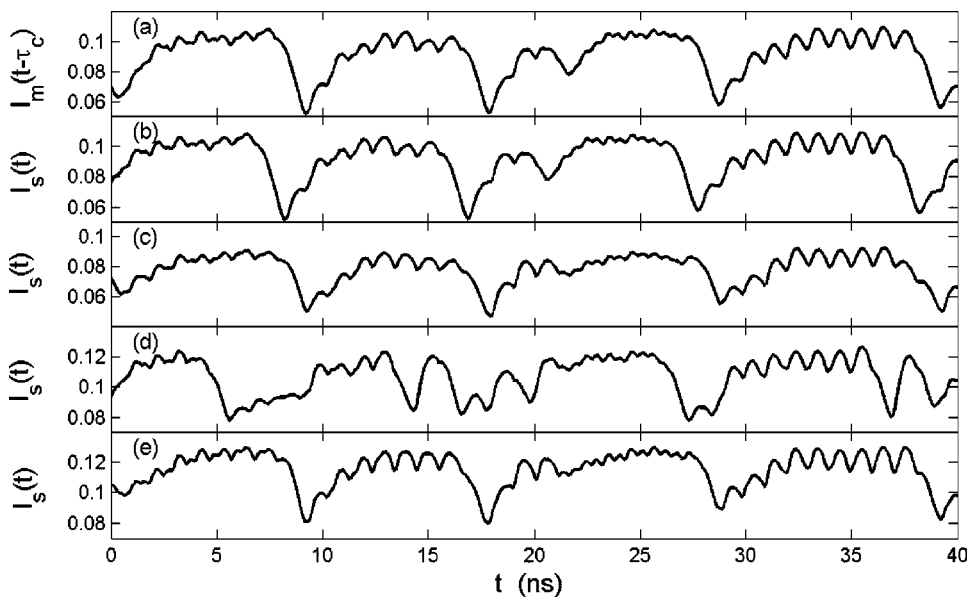


FIG. 10. Time traces of the time-averaged intensities. (a) Intensity of the master laser (lagged τ_c in time) for $\gamma_m = 10 \text{ ns}^{-1}$ and $\tau_{n,m} = 2 \text{ ns}$. Intensity of the slave laser for (b) $\eta = \gamma_m$, $\tau_{n,s} = \tau_{n,m}$; (c) $\eta = \gamma_m$, $\tau_{n,s} = 1.99 \text{ ns}$; (d) $\eta = \gamma_m$, $\tau_{n,s} = 2.01 \text{ ns}$; (e) $\eta = 13 \text{ ns}^{-1}$, $\tau_{n,s} = 2.01 \text{ ns}$. $\Delta\omega = 0$, all other parameters as in Fig. 4.

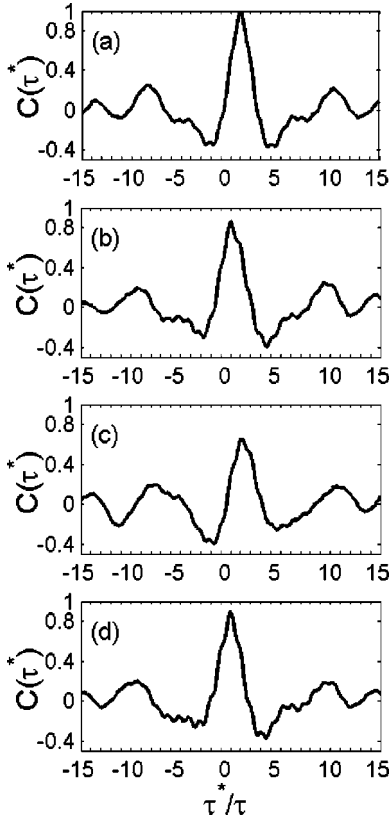


FIG. 11. Correlation coefficient as a function of the lag time (as explained in the text). (a), (b), (c), and (d) are for the same parameters as Figs. 10(b), 10(c), 10(d), and 10(e), respectively.

above which C_1 is larger than 0.95. We see that for the injection currents very close to threshold a good level of synchronization with lag time τ_c can be obtained with small injection rates (η close to γ_m), but for larger injection currents, much larger injection rates are needed.

In Fig. 12(b), good synchronization with a lag time $\tau_c - \tau$ occurs only when η is close to γ_m . Notice that for injection currents close to threshold, C_2 is relatively large even when η is much larger than γ_m . In the parameter region (low J , large η) both C_1 and C_2 are large, but $C_1 > C_2$ and it is isochronous and not anticipated synchronization that occurs. The large value of C_2 is due to the form of the chaotic intensity fluctuations in the LFF regime [the averaged intensity oscillates with a period nearly equal to τ in between dropouts, see Fig. 9(a)]. Notice also that there is an interval of injection currents (roughly speaking, for $1.1 < J_m/J_{th} < 1.3$), in which the anticipated synchronization is not stable.

Thus, we can conclude that only for injection currents close to threshold small parameter variations can lead to transitions between different synchronization regimes because the corresponding synchronization regions are close to each other in the parameter space. This is not possible with larger injection currents, since in that case the two types of synchronization occur in distant regions of the coupling strength.

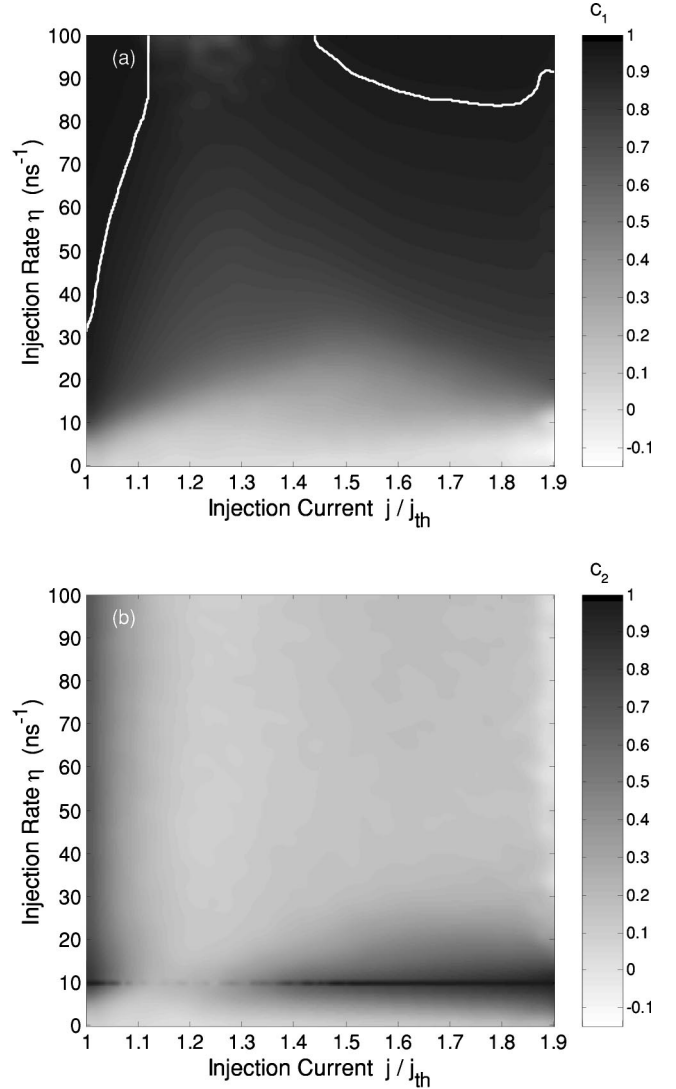


FIG. 12. Synchronization regions in the parameter space (injection current, optical coupling rate). (a) The value of C_1 is plotted. The white line corresponds to the threshold injection rate above which C_1 is larger than 0.95. For $1.15j_{th} < j < 1.4j_{th}$ approximately, the threshold injection rate is larger than 100 ns^{-1} (b) The value of C_2 is plotted. $\Delta\omega=0$, $\gamma_s=0$, all other parameters as in Fig. 4.

VI. SUMMARY AND CONCLUSIONS

We have numerically studied the synchronization of two unidirectionally coupled single-mode semiconductor lasers based on a Lang-Kobayashi-type model. The master laser is an external-cavity laser while for the slave laser we considered two configurations: an external-cavity slave laser (close-loop scheme) and a laser subjected only to the optical injection from the master laser (open-loop scheme).

Depending on the operating conditions two different types of synchronization can be found. Synchronization with a lag time τ_c , which corresponds to the synchronization of the slave optical field with the injected field (isochronous synchronization), and synchronization with a lag time $\tau_c - \tau$. In the latter case the optical field of the slave laser anticipates the injected field by an anticipation time equal to the round-

trip time τ in the external cavity of the master laser (anticipated synchronization).

We have studied the parameter regions in which the two synchronization regimes occur. We have shown that the chaotic synchronization with a lag time τ_c occurs in a similar parameter region in which stable cw injection-locking occurs. We have compared the degree of synchronization with an external-cavity slave laser (close-loop scheme) and with a solitary slave laser (open-loop scheme). We have observed that the synchronization quality is usually better in the close-loop scheme than in the open-loop scheme. However, when the slave laser is an external-cavity laser, the external mirror has to be carefully positioned, since small differences in the delay times strongly degrade the synchronization quality.

We have analyzed the synchronization regions in the parameter space (master feedback rate, injection rate), finding that an increase of the master feedback rate requires an increase of the injection rate in order to obtain a good synchronization. In the case of the close-loop scheme very good synchronization can occur even for a large value of γ_m , while in the case of an open-loop scheme the chaotic intensity produced by large feedback levels cannot be synchronized with feasible injection levels.

Finally, we have studied the transitions between the two synchronization regimes for an open-loop scheme, extending the results reported in Ref. [39]. We have shown that only for a injection current close to threshold small parameter variations can lead to transitions between the different synchronization regimes because the synchronization regions are close to each other in the parameter space. On the contrary, for large injection current transitions are not possible, since the two types of synchronization occur in distant regions of the coupling strength. We have also shown that not all parameter variations lead to a transition from one synchronization regime to the other, but only the parameter variations that increase the ratio between the injected power and the solitary slave laser output power. When a parameter variation decreases this ratio, a transition to the other synchronization regime does not occur and the synchronization is lost.

ACKNOWLEDGMENTS

C.M. is partially supported by PEDECIBA and CSIC (URUGUAY). C.R.M. is partially supported by the OCCULT project (IST-2000-29683) and the Spanish MCyT under projects CONOCE BFM2000-1108 and SINFIBIOS BMF2001.

-
- [1] H. Fujisaka and T. Yamada, *Prog. Theor. Phys.* **69**, 32 (1983).
 - [2] T. Yamada and H. Fujisaka, *Prog. Theor. Phys.* **70**, 1240 (1983).
 - [3] T. Yamada and H. Fujisaka, *Prog. Theor. Phys.* **72**, 885 (1984).
 - [4] L.M. Pecora and T.L. Carroll, *Phys. Rev. Lett.* **64**, 821 (1990).
 - [5] K.M. Cuomo and A.V. Oppenheim, *Phys. Rev. Lett.* **71**, 65 (1993).
 - [6] Y. Liu, P.C. De Oliveira, M.B. Danailov, and J.R. Rios Leite, *Phys. Rev. A* **50**, 3464 (1994).
 - [7] P. Colet and R. Roy, *Opt. Lett.* **19**, 2056 (1994).
 - [8] L.M. Pecora, T.L. Carroll, G.A. Johnson, D.J. Mar, and J.F. Heagy, *Chaos* **7**, 520 (1997).
 - [9] G.D. VanWiggeren and R. Roy, *Science* **279**, 1200 (1998).
 - [10] G.D. VanWiggeren and R. Roy, *Phys. Rev. Lett.* **81**, 3547 (1998).
 - [11] G. Perez and H.A. Cerdeira, *Phys. Rev. Lett.* **74**, 1970 (1995).
 - [12] K.M. Short, *Int. J. Bifurcation Chaos Appl. Sci. Eng.* **4**, 957 (1994).
 - [13] K.M. Short, *Int. J. Bifurcation Chaos Appl. Sci. Eng.* **6**, 367 (1996).
 - [14] K.M. Short and A.T. Parker, *Phys. Rev. E* **58**, 1159 (1998).
 - [15] J.B. Geddes, K.M. Short, and K. Black, *Phys. Rev. Lett.* **83**, 5389 (1999).
 - [16] C.R. Mirasso, P. Colet, and P. García-Fernández, *IEEE Photonics Technol. Lett.* **8**, 299 (1996).
 - [17] V. Annovazzi-Lodi, S. Donati, and A. Scire, *IEEE J. Quantum Electron.* **32**, 953 (1996).
 - [18] V. Annovazzi-Lodi, S. Donati, and A. Scire, *IEEE J. Quantum Electron.* **33**, 1449 (1997).
 - [19] P. Spencer, C.R. Mirasso, P. Colet, and A. Shore, *IEEE J. Quantum Electron.* **34**, 1673 (1998).
 - [20] J.P. Goedgebuer, L. Larger, and H. Porte, *Phys. Rev. Lett.* **80**, 2249 (1998).
 - [21] L. Larger, J.P. Goedgebuer, and F. Delorme, *Phys. Rev. E* **57**, 6618 (1998).
 - [22] V. Ahlers, U. Parlitz, and W. Lauterborn, *Phys. Rev. E* **58**, 7208 (1998).
 - [23] P. Spencer and C.R. Mirasso, *IEEE J. Quantum Electron.* **35**, 803 (1999).
 - [24] A. Sánchez-Díaz, C. Mirasso, P. Colet, and P. García-Fernández, *IEEE J. Quantum Electron.* **35**, 292 (1999).
 - [25] J.K. White and J.V. Moloney, *Phys. Rev. A* **59**, 2422 (1999).
 - [26] S. Sivaprakasam and K.A. Shore, *Opt. Lett.* **24**, 1200 (1999).
 - [27] Y. Takiguchi, H. Fujino, and J. Ohtsubo, *Opt. Lett.* **24**, 1570 (1999).
 - [28] H. Fujino and J. Ohtsubo, *Opt. Lett.* **25**, 625 (2000).
 - [29] H.F. Chen and J.M. Liu, *IEEE J. Quantum Electron.* **36**, 27 (2000).
 - [30] I. Fischer, Y. Liu, and P. Davis, *Phys. Rev. A* **62**, 011801 (2000).
 - [31] C. Masoller, *Phys. Rev. Lett.* **86**, 2782 (2001).
 - [32] I. Wedekind and U. Parlitz, *Int. J. Bifurcation Chaos Appl. Sci. Eng.* **11**, 1141 (2001).
 - [33] Y. Liu, H.F. Chen, J.M. Liu, P. Davis, and T. Aida, *Phys. Rev. A* **63**, 031802(R) (2001).
 - [34] S. Sivaprakasam, I. Pierce, P. Rees, P.S. Spencer, K.A. Shore, and A. Valle, *Phys. Rev. A* **64**, 013805 (2001).
 - [35] S. Sivaprakasam, E.M. Shahverdiev, P.S. Spencer, and K.A. Shore, *Phys. Rev. Lett.* **87**, 154101 (2001).
 - [36] F. Rogister, A. Locquet, D. Pieroux, M. Sciamanna, O. Deparis, P. Mégret, and M. Blondel, *Opt. Lett.* **26**, 1486 (2001).
 - [37] A. Locquet, F. Rogister, M. Sciamanna, P. Megret, and M. Blondel, *Phys. Rev. E* **64**, 045203(R) (2001).
 - [38] A. Locquet, C. Masoller, P. Mégret, and M. Blondel, *Opt. Lett.* **27**, 31 (2002).

- [39] I.V. Koryukin and P. Mandel, Phys. Rev. E **65**, 026201 (2002).
- [40] Y. Liu, Y. Takiguchi, P. Davis, T. Aida, S. Saito, and J.M. Liu (unpublished).
- [41] A. Murakami and J. Ohtsubo, Phys. Rev. A **65**, 033826 (2002).
- [42] J. Revuelta, C.R. Mirasso, P. Colet, and L. Pesquera, IEEE Photonics Technol. Lett. **14**, 140 (2002).
- [43] R. Lang and K. Kobayashi, IEEE J. Quantum Electron. **QE-16**, 347 (1980).
- [44] H.U. Voss, Phys. Rev. E **61**, 5115 (2000).
- [45] S. Tang and J.M. Liu, Opt. Lett. **26**, 596 (2001).
- [46] N.F. Rulkov, M.M. Sushchik, L.S. Tsimring, and H.D.I. Abarbanel, Phys. Rev. E **51**, 980 (1995).